International Journal of Optomechatronics

ISSN: 1559-9612 (Print) 1559-9620 (Online) Journal homepage: https://www.tandfonline.com/loi/uopt20

Dual Surgical Navigation Using Augmented and Virtual Environment Techniques

Sungmin Kim , Jaesung Hong , Sanghyun Joung , Atsushi Yamada , Nozomu Matsumoto , Sun I. Kim , Young Soo Kim & Makoto Hashizume

To cite this article: Sungmin Kim , Jaesung Hong , Sanghyun Joung , Atsushi Yamada , Nozomu Matsumoto , Sun I. Kim , Young Soo Kim & Makoto Hashizume (2011) Dual Surgical Navigation Using Augmented and Virtual Environment Techniques, International Journal of Optomechatronics, 5:2, 155-169, DOI: 10.1080/15599612.2011.581743

To link to this article: https://doi.org/10.1080/15599612.2011.581743

International Journal of Optomechatronics, 5: 155–169, 2011

ISSN: 1559-9612 print/1559-9620 online
DOI: 10.1080/15599612.2011.581743

Taylor & Francis
Taylor & Francis Group

DUAL SURGICAL NAVIGATION USING AUGMENTED AND VIRTUAL ENVIRONMENT TECHNIQUES

Sungmin Kim,[1] Jaesung Hong,[2] Sanghyun Joung,[3] Atsushi Yamada,[4] Nozomu Matsumoto,[5] Sun I. Kim,[1] Young Soo Kim,[6] and Makoto Hashizume[7]

[1]*Department of Biomedical Engineering, Hanyang University, Seoul, Korea*
[2]*Department of Robotics Engineering, Daegu Gyeongbuk Institute of Science and Technology, Daegu, Korea*
[3]*Department of Precision Engineering, The University of Tokyo, Tokyo, Japan*
[4]*Department of Computer Science and Engineering, Nagoya Institute of Technology, Nagoya, Japan*
[5]*Department of Otorhinolaryngology, Graduate School of Medical Sciences, Kyushu University, Fukuoka, Japan*
[6]*Department of Neurosurgery, College of Medicine, Hanyang University, Seoul, Korea*
[7]*Department of Advanced Medical Initiatives, Faculty of Medical Sciences, Kyushu University, Fukuoka, Japan*

To obtain additional depth and visual information in endoscopic surgery, a dual surgical navigation system using virtual reality (VR) and augmented reality (AR) techniques complementarily was developed. A VR environment was constructed in the default 3-D view of the navigation software and an AR environment was developed as a plug-in module. The spatial relationships among the target organ, endoscope, and surgical tools were visualized, and the visual information superimposing invisible organs on the endoscopic images was supplied using the AR environment. Phantom experiments and preliminary clinical application showed promising results for surgical navigation.

Keywords: augmented reality, endoscopic surgery, image guided surgery, surgical navigation, virtual reality

1. INTRODUCTION

Virtual reality (VR) technology and augmented reality (AR) technology have been employed in surgical navigation systems (Nakamura et al. 2010; Ukimura and Gill 2009; Liao et al. 2010; Tomikawa et al. 2010; Low et al. 2010). In particular, AR technology allows for radiographic images to be superimposed on real

Address correspondence to Jaesung Hong, Daegu Gyeongbuk Institute of Science and Technology, Department of Robotics Engineering, Daegu, Republic of Korea. E-mail: jhong@dgist.ac.kr

NOMENCLATURE

${}^{CM}T_C$	transformation matrix of the endoscopic camera from the marker attached to the endoscopic camera	${}^{P}T_{CM}$	transformation matrix of the marker attached to the endoscopic camera from the position sensor
${}^{CP}T_C$	transformation matrix of the endoscopic camera from the calibration pattern	${}^{P}T_{CP}$	transformation matrix of the position sensor to the calibration pattern
${}^{P}T_C$	transformation matrix of the endoscopic camera from the position sensor		

endoscopic or microscopic images, which provides valuable information about the position of target sites or important vessels inside the organs of interest. A number of studies have been performed to improve accuracy and visualization using these techniques. Kawamata et al. (2002) used the AR technique in endoscopic surgery. A wire-frame model was overlaid on raw endoscopic images to provide spatial information. The wire-frame model was registered manually and the color of the wire-frame model indicates the distance between the endoscope and the organ. Su et al. (2009) applied AR to robot-assisted laparoscopic surgery. A 3-D surface model was overlaid on the real-time stereo-endoscope during robot-assisted laparoscopic partial nephrectomy. A manual registration method was applied for coarse alignment and a surface-tracking technique was employed for fine alignment. Sugimoto et al. (2010) applied mixed reality (MR) to endoscopic surgery. MR refers to a mixture of VR and AR that complement each other. Using the MR environment, the organs inside the patient can be projected onto the skin of the patient to display the spatial relationships between the endoscope and the organs.

On the contrary, VR-based surgical navigation is common in commercially available systems, the StealthStation (Medtronics, Inc., MN, US) and VectorVision (BrainLab, Inc., NJ, US) are widely used commercialized systems (Morioka et al. 1999; Gumprecht, Widenka, and Lumenta 1999). It can provide accurate positioning of surgical tools on radiographic images, but surgeons cannot see the crucial endoscope or microscope screen while they are looking at the VR-based navigation. Therefore AR navigation can be considered more useful in this respect.

One of the key issues related to AR surgical navigation is the lack of depth information in the endoscopic images, even if overlaid target organ models are supplied during surgery. This concern is common among surgeons who have been using such endoscopic surgical navigation systems (Sugimoto et al. 2010; Su et al. 2009; Kawamata et al. 2002). Ukimura et al. (2009) and Kawamata et al. (2002) have attempted to deliver the necessary depth information using color coded methods to overlay target objects. However, the color of translucent images may either be unclear or interfere with the background endoscopic images. There have also been several studies of systems that use 3-D endoscopes to provide 3-D depth information (Mitchell et al. 2002; Mountney et al. 2006; Mourgues, Devernay, and Coste-Maniere 2001; Mueller-Richter et al. 2003). Moreover, there are several commercial systems, such as 3-D/2-D endoscopic imaging systems for the da Vinci surgical

system (Olympus Co. Ltd, Tokyo, Japan), wedge prism 3-D endoscope (Shinko Optical Co. Ltd, Tokyo, Japan), and Wasol's 3-D endoscope (Wasol, Seoul, Korea). Surgeons, however, should wear special glasses during this type of surgery, and the system is not popular yet because of its complexity, high cost, and inherently causing fatigue in surgeons that use it.

In this study, by using VR navigation and synchronizing it with AR navigation, we attempted to resolve the depth problem. We developed a surgical navigation system using AR and VR techniques simultaneously. These two techniques are used in a complementary manner and assist surgeons by providing additional depth and width information for the surgical area.

In the proposed system, an optical position sensor or an electromagnetic sensor detects the position of the endoscope and the surgical instruments. Based on the predetermined camera calibration parameters, a rendered 3-D object is placed on the endoscopic image with an AR technique. At the same time, the positions of the endoscope and the surgical instruments are also displayed in virtual 3-D space, i.e., a VR environment. Finally, the surgeon can perform the surgery referring to the augmented endoscopic images. Whenever the surgeon wants to know the distance to the target overlaid on the endoscopic image, he can confirm it on a VR view that is synchronized with an AR view. To verify the performance of the proposed dual navigation system, phantom experiments were conducted in several conditions using either CT or MR image volume data and the Polaris Vicra or the Aurora systems as position sensors. A preliminary clinical application analysis was also conducted in a cochlear implant surgery. Phantom experiments and a preliminary clinical application test were conducted to confirm the feasibility of this proposed surgical system.

2. METHODS FOR DUAL SURGICAL NAVIGATION

2.1. System Architecture of Dual Surgical Navigation

3D Slicer (Brigham and Women's Hospital, Boston, USA) is a free open-source software that was used as a basic platform software in this research. The proposed system consists of 3D Slicer, a tracker client, and a registration client (Figure 1).

In this study, a VR environment was implemented in the default 3-D view of 3D Slicer, and an AR environment was developed as a plug-in module (VideoOverlay) and implemented as a child window of the 3D Slicer. Volume data and surface model data were shared in both environments via 3D Slicer. The position information for the target organ and the surgical tools were also shared in the system.

To detect and track the surgical tools, such as the endoscope and forceps, an optical position sensor (Polaris Vicra, NDI, Waterloo, Canada) and an electromagnetic sensor (Aurora, NDI, Waterloo, Canada) were employed. Although the optical system provides better accuracy and a wireless connection, it cannot recognize the tool when the infrared is blocked by any person or machine located between the camera and the tool. On the other hand, the electromagnetic system is less accurate and needs a wired connection, but it can be used even in an environment where some

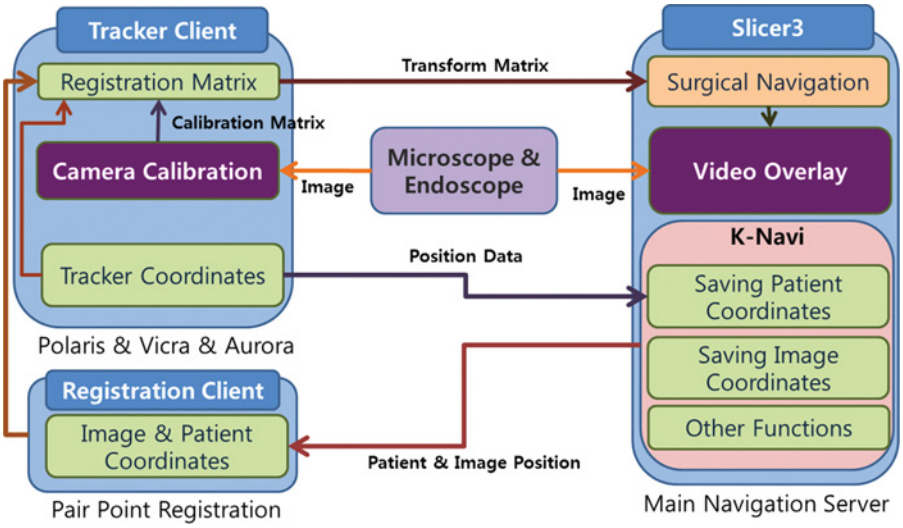

Figure 1. The proposed system consists of the 3D Slicer, a tracker client, and a registration client.

obstacles exist between the sensor and surgical tools. For the tracking of a flexible endoscope, the electromagnetic sensor might be more appropriate because the end tip of the endoscope is located inside the body. However, the accuracy of the electromagnetic sensor is worse than the optical position sensor, so selecting the proper sensor system must be done while considering the surgery being performed.

The proposed system is capable of accepting these two sensor systems through the tracker client module. We used both sensors in these experiments for evaluation. To perform surgical navigation using AR and VR, image to patient (real-space) registration, camera calibration and 3-D data rendering techniques are essential. The registration client has roles for image to patient registration, and the tracker client has roles for managing position sensors and camera calibration. Finally, VR- and AR-based dual navigation was integrated and implemented in the VideoOverlay module of 3D Slicer.

2.2. VR-Based Navigation

For the registration between image and patient, the paired point registration method (Arun and Blostein 1987; Germano 2001; Nottmeier and Crosby 2007; West et al. 2001; Challis 1995) was applied in the registration client (Hong and Hashizume 2010). The paired point registration method computes a transformation matrix using at least three paired points between the patient and the image. The points can be specified on the images by the manipulation of a computer mouse, and the coordinates of the corresponding points on the patient's body were also obtained using the probe device of an optical or an electromagnetic position sensor. Using VR-based navigation, the positional relationship between the target organs, endoscope, and surgical tools can be presented intuitively.

2.3. AR-Based Navigation

To support endoscopic surgery with visual information superimposing invisible organs on the endoscopic images, an AR technique was applied. First, camera calibration was required to obtain the parameters of the endoscopic camera (Figure 2). Through camera calibration procedures, intrinsic parameters, extrinsic parameters, and lens distortion coefficients were obtained. For camera calibration, Zhang's method, which is widely used in the computer vision research field, was implemented using a computer vision library, OpenCV (Intel 2000; Bradski and Kaehler 2008).

Using the results of camera calibration, a virtual camera model and rendering environment are constructed and the 3-D model of the target tumors or important vessels inside the organs of interest can be rendered. Because the rendering is conducted with respect to the parameters of the endoscopic camera, the rendered results mimic the shape and size of the real object. In addition, because the rendering is performed with respect to the spatial relationship between the endoscope and organs, the position and orientation of the rendered model coincide with the real target object.

2.3.1. Camera calibration. For camera calibration, a camera calibration module was implemented in the tracker client (Figure 3*a*). This camera calibration module conducts camera calibration with endoscopic images, tracking data, and calibration patterns. The graphical user interface (GUI) of the client software was constructed with the Microsoft foundation class (MFC) library and the main functions of camera calibration were implemented with the OpenCV library.

To conduct camera calibration, a calibration pattern is captured 9 times in various directions and orientations. Using those captured images, intrinsic

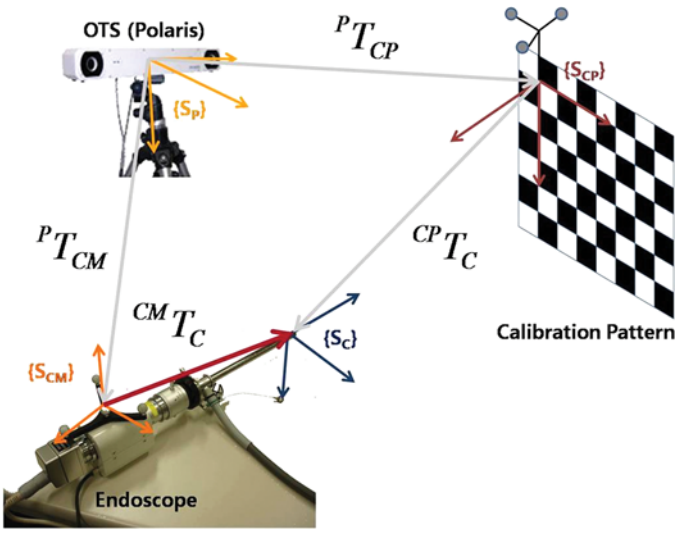

Figure 2. Concept of camera calibration. Camera calibration is required to obtain the parameters of the endoscope, which are intrinsic and extrinsic parameters and lens distortion coefficients. Using the results of camera calibration, the relationship between the coordinate system of the position sensor and the coordinate system of the real endoscopic camera can be computed.

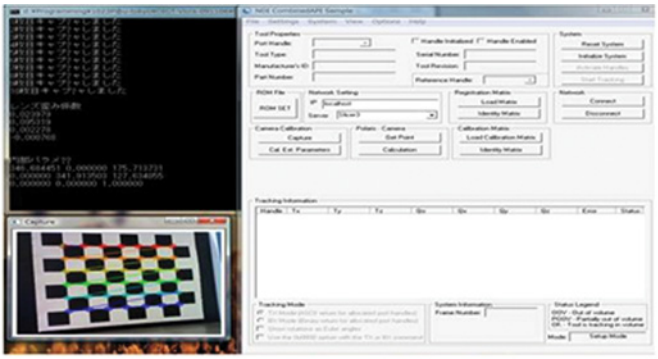

(*a*)

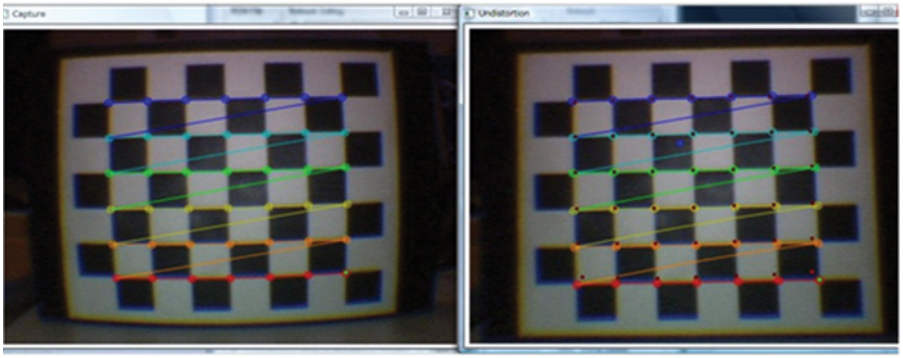

(*b*)

Figure 3. For camera calibration, a camera calibration module was implemented in the tracker client (*a*). After camera calibration, correcting endoscopic image was conducted with those calculated parameters (*b*).

parameters and lens distortion coefficients are computed using Zhang's method (Zhang 2000). After that, the camera image is undistorted with the calculated parameters (Figure 3*b*). The extrinsic parameters are also calculated with respect to the spatial relationship between the calibration pattern and the endoscopic camera. The spatial relationship can be obtained with the captured, undistorted endoscopic image.

When each undistorted endoscopic image is captured, the corner point of the calibration pattern is detected, and 3-D reconstructed coordinates are computed. Using the reconstructed coordinates, a transformation matrix of the endoscopic camera from the calibration pattern, ${}^{CP}T_C$, is computed. The transformation matrix is comprised of the extrinsic parameters of the camera, which are required to render the 3-D model with respect to the spatial relationship between the real endoscopic camera and the organs.

At the same time, a transformation matrix of the marker attached to the endoscopic camera from the position sensor, ${}^{P}T_{CM}$, and a transformation matrix, ${}^{P}T_{CP}$, for the position sensor to the calibration pattern are obtained by measurement with

the position sensors. From a series of transformation matrices, the relationship between the coordinates of the endoscopic camera and the coordinates of the marker attached to the endoscopic camera, ${}^{CM}T_C$, is finally calculated.

From the obtained transformation matrix, ${}^{P}T_C$ is calculated as follows:

$$ {}^{P}T_C = {}^{P}T_{CP}\ {}^{CP}T_C. \tag{1} $$

Because ${}^{P}T_{CM}$ is also obtained by the Polaris, ${}^{CM}T_C$ is calculated as follows:

$$ {}^{CM}T_C = {}^{P}T_{CM}\ {}^{TP}T_C = {}^{CM}T_P\ {}^{P}T_C. \tag{2} $$

Using the ${}^{CM}T_C$ matrix, a transformation matrix of the endoscopic camera from the Polaris can be calculated as follows:

$$ {}^{P}T_C = {}^{P}T_{CM}\ {}^{CM}T_C. \tag{3} $$

Using the calculated ${}^{P}T_C$ matrix, the surgical navigation system can track the markers attached to the endoscope.

2.3.2. Overlaying 3D data on the endoscopic camera image. Rendering 3-D data is implemented with the Visualization ToolKit (VTK, Kitware Inc., NY, USA) on the 3D Slicer. In this study, 3-D volume data from CT and MR was acquired. For 3-D volume rendering, the surgical target organs are segmented and volume rendering is conducted with a 3-D texture mapping method. Because the 3-D texture mapping method is a hardware accelerated rendering method, the result of volume rendering is far faster than with any other software-based rendering such as ray casting. Volume rendering, however, proved to be inappropriate in our study because it has a time delay depending on the volume size, and is thus not suitable for multi-object rendering.

Alternatively, 3-D surface models are generated from the segmented volumes of the target organ in the 3D Slicer. Using those models, fast 3-D surface rendering is conducted. Implementing multiple object rendering and opacity control are possible; thus when there are multiple organs that are important considerations for the surgery they can be presented simultaneously on the endoscopic image.

For the augmented endoscopic images, a virtual graphic environment is constructed. In the virtual environment, there are 3-D data (volume data or 3-D surface model data), endoscopic image view plane, and the endoscopic camera. First, using the intrinsic parameters of the endoscopic camera, the relationship between the endoscopic image plane and the endoscopic camera is determined. This means that the plane is located at the center of the previous 3-D virtual space, and then the position and orientation of the endoscopic camera is determined relatively with respect to the intrinsic parameters. The endoscopic camera model mimics a general pinhole camera model. Using the data from the position sensor system, a transformation matrix that presents the relationship between the 3-D surface model and the virtual endoscopic camera model is calculated, and finally a 3D surface model is overlaid on the raw endoscopic image (Figure 4).

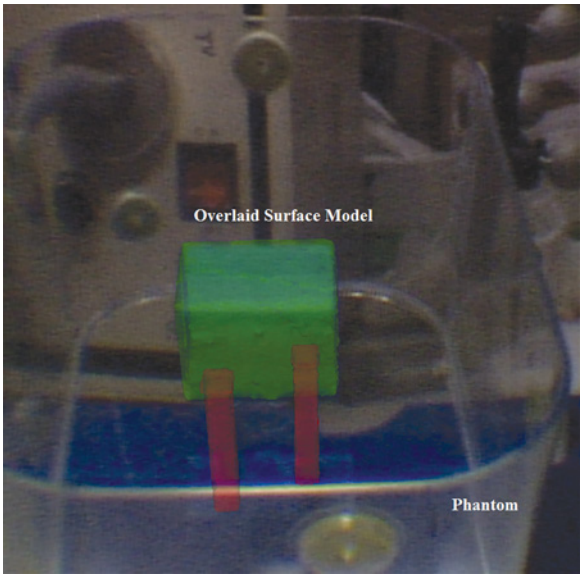

Figure 4. Overlaying the surface model on endoscopic images. The surface model is overlaid accurately on the endoscopic image (see the phantom in Figure 5).

2.4. Phantom Experiments

To evaluate the accuracy of this system, a phantom experiment was conducted. A 1.5 cm × 2 cm × 3 cm plastic cube representing the target was placed in a transparent acrylic box (Figure 5). CT images with 1.0 mm slices were acquired for this phantom. T1-weighted MR imaging was also done with 3.0 mm slices. Since the phantom itself cannot be imaged in MR, we filled the box with pure water, and obtained negative images for the cube.

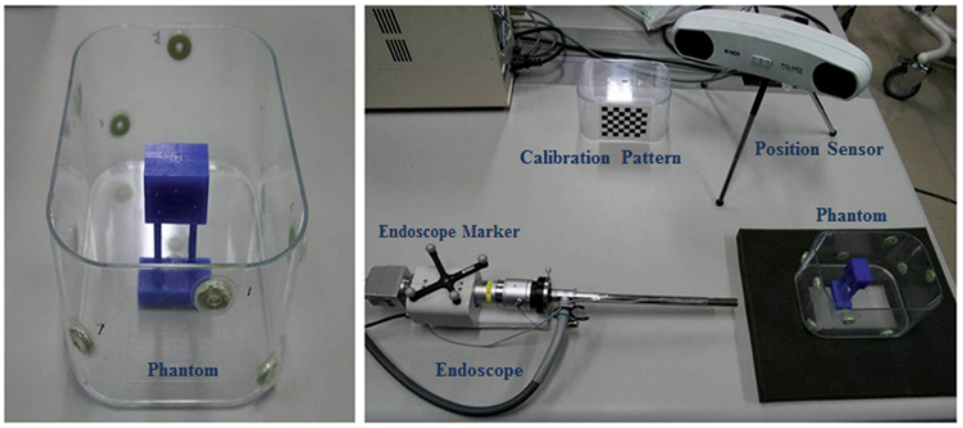

Figure 5. The phantom for evaluation (left) and the experimental setup for evaluation (right).

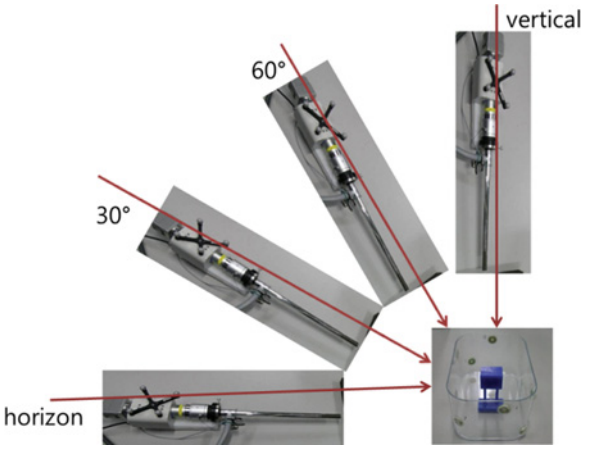

Figure 6. Errors between the overlaid phantom and the real object in various endoscopic angles from horizontal to vertical were measured. Translational, angular and area errors were measured at different endoscopic angles.

From the CT and MR images, the target cube part was segmented by a threshold, and a surface model was generated. Finally, the surface model was rendered on the endoscopic image.

For the experiments, a 10-mm straight vision laparoscope was used. In addition, the Polaris Vicra optical position sensor and the Aurora electromagnetic position sensor were employed.

We measured the error between the overlaid phantom and the real object in various endoscopic angles from the horizontal to the vertical (Figure 6). According to the angles, translational, angular, and area errors were measured. The endoscopic angles were 0, 30, 60, 90 degrees, and the experiments were conducted 9 times for each endoscopic angle.

The translational error was defined as the difference between the centroid of the real phantom and the overlaid result, and the angular error was defined as the angle difference between the real phantom and the overlaid model. The area error

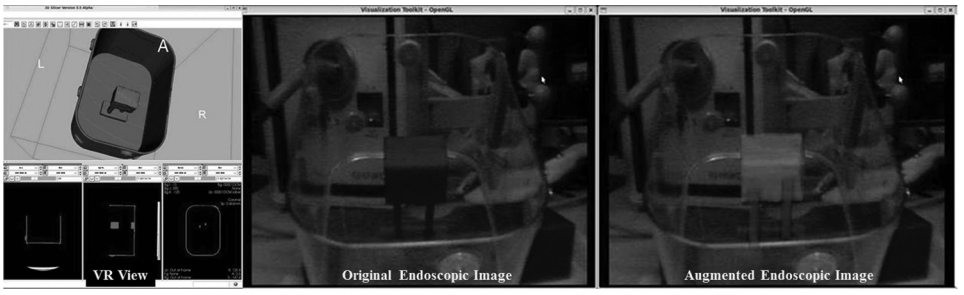

Figure 7. The left image is a 3-D rendering view (VR view) and the middle is the original endoscopic image. The right image shows the resulting overlaid 3-D surface model data on the endoscopic image. Evaluation was conducted using the raw endoscopic images and the augmented endoscopic images.

(*a*) An Adapter for Microscope (*b*) Setting up for Microscopic Surgery

Figure 8. To attach the markers, an adapter was designed with CAD software and manufactured with a CNC milling machine (*a*). After sterilizing the adapter and markers, those parts were set up on the microscope (*b*).

was defined as the difference in area between the real phantom and the overlaid result in the endoscopic images (Figure 7).

2.5. Clinical Application

We applied the proposed dual navigation system to a cochlear implant surgery. Instead of the endoscope, a surgical microscope was used. The Polaris system was employed as a position sensor, and the sterilized markers were attached to the

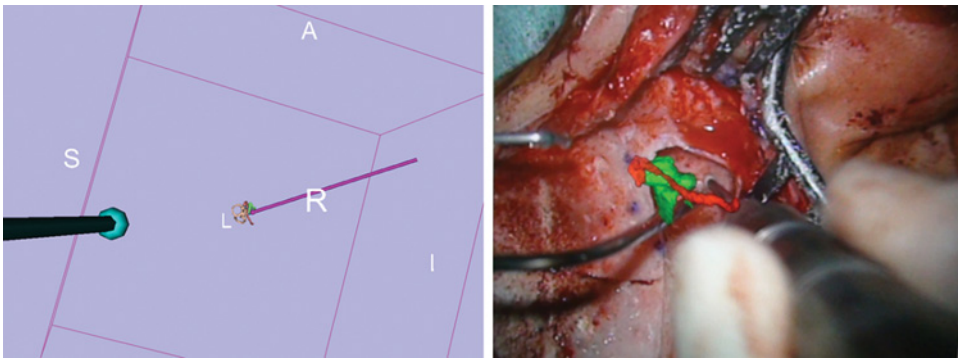

Figure 9. Multiple organs were presented simultaneously on the endoscopic image. During the surgery, segmented multiple objects, a microscope, and a surgical tool were rendered in the VR environment (left) and a synchronized augmented microscopic image was generated with an AR technique (right).

microscope body. To attach the markers, an adapter was designed with CAD software and manufactured with a CNC milling machine (Figure 8*a*). After sterilizing the adapter and markers, those parts were fixed onto the microscope (Figure 8*b*). The cochlea and facial nerve were segmented and surface models were generated preoperatively. Camera calibration of the surgical microscope was also conducted in the preoperative time. Using previous results, surface models were overlaid on the microscopic images (Figure 9).

3. RESULTS

A dual surgical navigation system with VR and AR techniques were proposed and tested in simulated and clinical environments. To evaluate the performance of this dual surgical navigation system that uses both VR and AR, phantom experiments were conducted under several experimental conditions. The preliminary feasibility of our system in clinical applications was evaluated in a surgical procedure that was performed in the operating room.

For phantom experiments, CT and MR image volume data were employed, and the Polaris Vicra and Aurora systems were applied. To account for various surgical situations, the experiments were conducted using various endoscopic angles. Through phantom experiments, the accuracy of the overlaid results was measured (translational error, angular error, and area error). Figure 10 shows the overall errors of distance, angle and area, respectively. The graphs show that the Polaris Vicra system has less error than the Aurora system and the experiments with CT data are more accurate than the experiments with MR data. This is because the

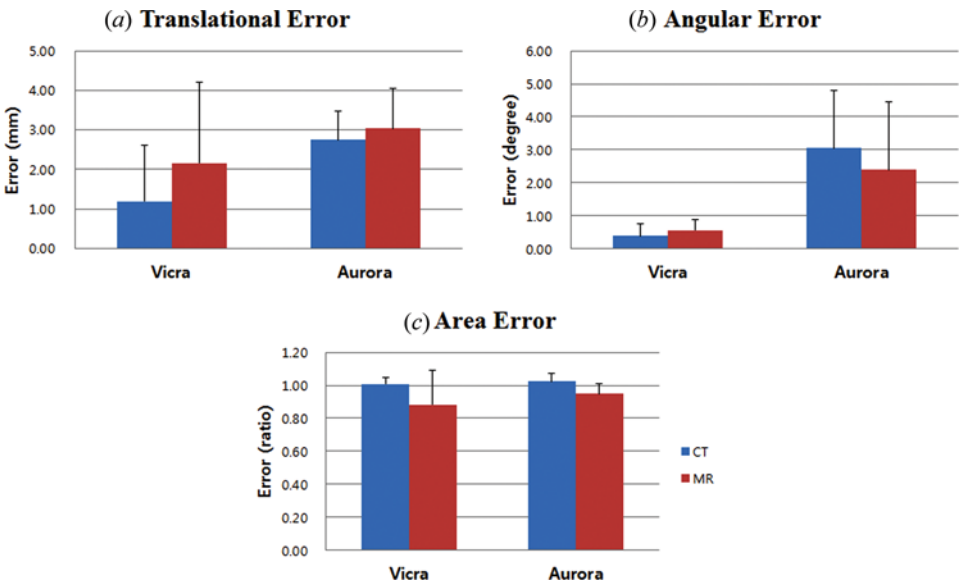

Figure 10. The experiments were performed with CT and MR image volume data using the Polaris Vicra or the Aurora system as a position sensor. Errors are presented in graphs that show translational error (*a*), angular error (*b*) and area error (*c*).

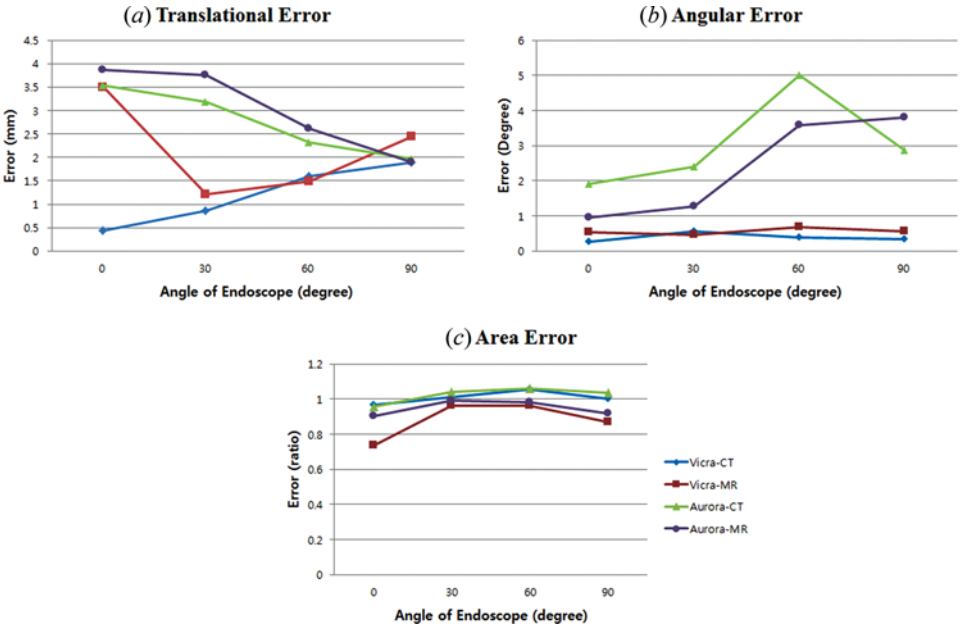

Figure 11. The evaluation results according to the varied angles of the endoscopic camera are presented graphically. The graphs show translational errors (*a*), angular errors (*b*) and area errors (*c*).

Polaris system, which is an optical position sensor, performs better in surgical navigation than the Aurora system, which is an electromagnetic position sensor. Moreover, CT data has less distortion than MR data. For these reasons, navigation with CT data using the Polaris Vicra system shows better performance than the other conditions.

In addition, the trend in error was observed for measurements taken with endoscopic camera angles that were varied from the horizontal angle to the vertical angle. The results according to the angle of the endoscopic camera are presented graphically in Figure 11. When the Aurora system was used, the translational errors decreased. On the other hand, the results of the Polaris Vicra had an increasing trend in error size. In the errors of angle and area, the errors using the Aurora system were larger than those using the Polaris Vicra system for all endoscopic camera angles.

A preliminary clinical application analysis of this system was conducted. Numerical evaluation was not performed; we only confirmed the potential feasibility of this system in clinical applications. The surgeon who performed the cochlear implant surgery was satisfied with the results of this system.

4. DISCUSSION

We have developed a dual surgical navigation system for endoscopic surgery using VR and AR techniques complementarily to obtain additional depth and visual information for organs. With a VR environment, the spatial relationships among the

target organ, endoscope and surgical tools are visualized. With an AR environment, augmented endoscopic images overlaying invisible organs on the raw endoscopic images support the surgery. Surgeons can recognize and better understand the surgical environment around the target, and perform their surgeries more safely and accurately.

In phantom experiments, the overall error was less than 2 mm with CT images and an optical position sensor. Relatively high errors were observed with MR images and an electromagnetic sensor. In addition, trends in errors according to endoscopic camera angles were observed to account various surgical situations. In translational errors, the results of the Aurora system had a downward trend while the results of the Polaris Vicra system had an upward trend. In the errors of angle and area, moreover, the results of the Aurora system had significantly larger errors than the Polaris Vicra. These error trends according to the endoscopic angles were considered to be a matter of recognition performance and the detectable volume area of the position sensors. Furthermore, the positions of the detectable markers also affected the error trends. When the Aurora system was used the markers were attached at the end of the laparoscope, resulting in a shorter distance between the electromagnetic field generator and marker in near-vertical angle cases, and a shorter distance between the electromagnetic field generator and marker has better accuracy. For this reason, the errors using the Aurora system tended to decrease as the endoscopic angle increased. Moreover, magnetic distortion occurred because the end of the laparoscope is made from metallic material and the marker was attached onto the metallic body, and this affected the experimental results. Despite the relatively better results in near-vertical endoscopic angles achieved using the Aurora system, the Aurora system had larger errors overall compared to the Polaris Vicra system. When the Polaris Vicra system was used the marker was attached to the body of the laparoscope, resulting in a marker on the boundary region of the detectable volume in near-vertical endoscopic angles. This affected the error trends, with the larger errors occurring when the endoscopic angle was near-vertical and smaller errors occurring with horizontal endoscopic angles.

In a clinical setting, our dual navigation system was applied to a cochlear implant surgery. Although there were some problems because this system was applied to a surgical microscope instead of an endoscope, the AR and VR navigations were synchronized well. Although this was a preliminary study, this clinical application analysis confirmed the feasibility of such a system in clinical environments.

In our study, the displacement of soft organs was not considered. The reason we selected cochlear implant surgery as a clinical application is that the surgery has nothing to do with the organ deformation problem. It is clear for hard tissue organs that there is no deformation before or after the imaging. For this reason, cochlear implant surgery is very proper target surgery for our system. However, the displacement of soft organs caused by inflating with carbon dioxide or by the timing of image acquisition should be resolved before applying this system to abdomen area.

The evaluations of this study were oriented to the AR overlay accuracy rather than the quantitative analysis about the dual navigation, because the nature of the study and following evaluation is closer to qualitative aspects. If only the AR overlay accuracy is guaranteed, it is apparent that the dual navigation is more beneficial than

single VR or AR navigation. In addition, the surgeons who have observed and used in the clinical study declared the usefulness of the dual navigation system. From these points of view, the proposed system is considered to have significant advantages compared to conventional systems.

5. CONCLUSIONS

By combining VR and AR technologies, an effective surgical navigation system that can provide additional depth information about invisible organs was proposed. Performance was verified in phantom experiments. It was also revealed that it is important to select proper imaging modalities and the proper type of position sensors for surgical navigation systems. The results of a preliminary clinical application of this system showed clinical feasibility. We expect that this dual navigation system could be a great help in particularly difficult surgeries using camera-based images.

ACKNOWLEDGMENTS

The main part of this work was performed, when Sungmin Kim and Jaesung Hong worked at Kyushu University.

This work was partially supported by the Korea Research Foundation Grant funded by the Korean Government (KRF-2008-621-D00062), and by the research fund of NEDO P10003 ''intelligent surgical instrument project,'' Japan.

REFERENCES

Arun, K. S. and S. D. Blostein. 1987. Least-square fitting of two 3-D point sets. *IEEE Trans Pattern Anal. Mach. Intell.* 9: 698–700.

Bradski, Gary R. and Adrian Kaehler. 2008. *Learning OpenCV: [computer vision with the OpenCV library]*. Sebastopol, CA: O'Reilly.

Challis, J. H. 1995. A procedure for determining rigid body transformation parameters. *J. Biomech.* 28 (6): 733–737.

Germano, I. M., ed. 2001. *Advanced techniques in image-guided brain and spine surgery*. New York: Thieme.

Gumprecht, H. K., D. C. Widenka, and C. B. Lumenta. 1999. BrainLab VectorVision Neuronavigation System: Technology and clinical experiences in 131 cases. *Neurosurgery* 44 (1): 97–104; discussion 104–105.

Hong, J. and M. Hashizume. 2010. An effective point-based registration tool for surgical navigation. *Surg. Endosc.* 24 (4): 944–948.

Intel. 2000. *Open Source Computer Vision Library (Reference Manual)*. http://www.cs.unc.edu/Research/stc/FAQs/OpenCV/OpenCVReferenceManual.pdf (accessed May 12, 2011).

Kawamata, T., H. Iseki, T. Shibasaki, and T. Hori. 2002. Endoscopic augmented reality navigation system for endonasal transsphenoidal surgery to treat pituitary tumors: technical note. *Neurosurgery* 50 (6): 1393–1397.

Liao, H., H. Ishihara, H. H. Tran, K. Masamune, I. Sakuma, and T. Dohi. 2010. Precision-guided surgical navigation system using laser guidance and 3D autostereoscopic image overlay. *Comput. Med. Imaging Graph.* 34 (1): 46–54.

Low, D., C. K. Lee, L. L. Dip, W. H. Ng, B. T. Ang, and I. Ng. 2010. Augmented reality neurosurgical planning and navigation for surgical excision of parasagittal, falcine and convexity meningiomas. *Br. J. Neurosurg.* 24 (1): 69–74.

Mitchell, P., I. D. Wilkinson, P. D. Griffiths, K. Linsley, and J. Jakubowski. 2002. A stereoscope for image-guided surgery. *Br. J. Neurosurg* 16 (3): 261–266; discussion 267–268.

Morioka, T., S. Nishio, K. Ikezaki, Y. Natori, T. Inamura, H. Muratani, M. Muraishi, K. Hisada, F. Mihara, T. Matsushima, and M. Fukui. 1999. Clinical experience of image-guided neurosurgery with a frameless navigation system (StealthStation). *No. Shinkei Geka* 27 (1): 33–40.

Mountney, P., D. Stoyanov, A. Davison, and G. Z. Yang. 2006. Simultaneous stereoscope localization and soft-tissue mapping for minimal invasive surgery. *Med. Image Comput. Comput. Assist. Interv.* 9 (Pt 1): 347–354. *Proceedings of ISAR*: 191–192.

Mourgues, F, F. Devernay, and E. Coste-Maniere. 2001. 3-D reconstruction of the operating field for image overlay in 3D-endoscopic surgery.

Mueller-Richter, U. D., A. Limberger, P. Weber, W. Spitzer, and M. Schilling. 2003. Comparison between three-dimensional presentation of endoscopic procedures with polarization glasses and an autostereoscopic display. *Surg. Endosc.* 17 (3): 502–504.

Nakamura, K., Y. Naya, S. Zenbutsu, K. Araki, S. Cho, S. Ohta, N. Nihei, H. Suzuki, T. Ichikawa, and T. Igarashi. 2010. Surgical navigation using three-dimensional computed tomography images fused intraoperatively with live video. *J. Endourol.* 24 (4): 521–524.

Nottmeier, E. W. and T. L. Crosby. 2007. Timing of paired points and surface matching registration in three-dimensional (3-D) image-guided spinal surgery. *J. Spinal Disord Tech.* 20 (4): 268–270.

Su, L. M., B. P. Vagvolgyi, R. Agarwal, C. E. Reiley, R. H. Taylor, and G. D. Hager. 2009. Augmented reality during robot-assisted laparoscopic partial nephrectomy: Toward real-time 3D-CT to stereoscopic video registration. *Urology* 73 (4): 896–900.

Sugimoto, M., H. Yasuda, K. Koda, M. Suzuki, M. Yamazaki, T. Tezuka, C. Kosugi, R. Higuchi, Y. Watayo, Y. Yagawa, S. Uemura, H. Tsuchiya, and T. Azuma. 2010. Image overlay navigation by markerless surface registration in gastrointestinal, hepatobiliary and pancreatic surgery. *J. Hepatobiliary Pancreat Surg.* 17 (5): 629–636.

Tomikawa, M., J. Hong, S. Shiotani, E. Tokunaga, K. Konishi, S. Ieiri, K. Tanoue, T. Akahoshi, Y. Maehara, and M. Hashizume. 2010. Real-time 3-dimensional virtual reality navigation system with open MRI for breast-conserving surgery. *J. Am. Coll. Surg.* 210 (6): 927–933.

Ukimura, O. and I. S. Gill. 2009. Image-fusion, augmented reality, and predictive surgical navigation. *Urol. Clin. North Am.* 36 (2): 115–123, vii.

West, J. B., J. M. Fitzpatrick, S. A. Toms, C. R. Maurer, Jr., and R. J. Maciunas. 2001. Fiducial point placement and the accuracy of point-based, rigid body registration. *Neurosurgery* 48 (4): 810–816; discussion 816–817.

Zhang, Z. Y. 2000. A flexible new technique for camera calibration. *IEEE Trans Pattern Anal. Mach. Intell.* 22 (11): 5.